Note: this paper is originally published in Advanced Experimental Mechanics issued by the Japanese Society for Experimental Mechanics.

Analysis of Creep Behavior of Bending Beam Load Cell

Thomas P. KIEFFER

Vishay Precision Group – Micro-Measurements, Raleigh, NC USA

(*Received 14 November 2017; received in revised form 21 March 2018; accepted 1 April 2018*)

Abstract: This paper provides an analysis of transducer creep by quantifying the individual creep contributions of the counterforce; strain gage backing and adhesive; and strain gage resistive metal foil. The analysis utilizes 14 plane-strain finite element models of a 30-kg aluminum bending beam load cell instrumented with strain gages made with Cu-Ni (constantan) and Ni-Cr (modified Karma) resistive metal foil and with end loop lengths varying from 0.09 to 0.30 mm. Physical measurement of transducer creep is also performed using dead-weight load application of aluminum bending beam load cells corresponding to the finite element models. This paper demonstrates good correlation between finite element analysis and dead-weight creep test results: minimum transducer creep of -22 and -30 μV/V is achieved for strain gages made of Ni-Cr and Cu-Ni resistive metal foil with end loop lengths of 0.18 and 0.20 mm, respectively. These results are consistent with the analysis in that the relative lengths of the end loops for the two resistive metal foils correspond with their relative creep contributions.

Keywords: Transducer creep, Strain gage creep, Metal foil strain gage, Finite element model, Dead-weight testing

1. Introduction

Strain gage based transducers are used to measure a variety of physical parameters such as weight, force, mass, torque, pressure, displacement, and acceleration. Transducer creep is a well-known phenomenon that tends to limit the accuracy of these measurements particularly with load cell transducers used in weighing applications. After applying a constant weight, the load cell output changes with time as depicted in Fig. 1 due to the combined, time-dependent relaxation (creep) of the individual materials of construction, principally the weight-bearing structure of the load cell (the counterforce); the resistive metal foil of the strain gages; and the bonding adhesive and electrically insulating backing located between the counterforce and the foil. There are internationally recognized standards such as OIML R60 (Organisation Internationale de Metrologie Legale) which prescribe the maximum combined error for specific accuracy classes of load cells used in legal-for-trade applications. The 3000D accuracy class allows 1 part error in 3000 divisions of measurement (0.033%) [1].

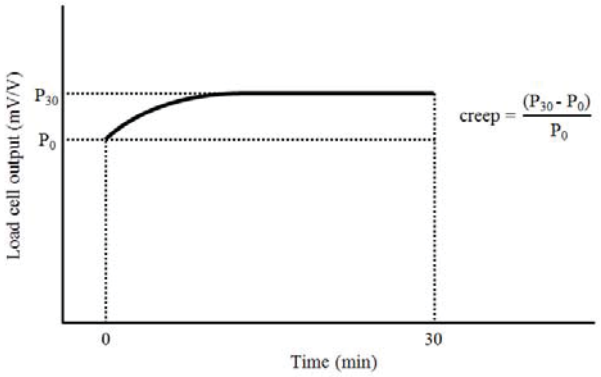

Fig. 1 Conceptual depiction of time-varying load cell creep phenomenon and calculation of creep magnitude

The techniques used by strain gage and load cell manufacturers to minimize creep are well known. The most common technique involves changing the lengths of the end loop portions of the strain gages. By shortening the strain gage end loops the load cell creep tends to move in a negative direction, and conversely by lengthening the strain gage end loops the load cell creep tends to move in a positive direction. Other techniques used to minimize creep have been addressed in the patent literature such as changing the angular orientation of the end loop to the grid line [2]; changing the shape of the end loop [3]; and compensating positive and negative creep components of individual arms of the Wheatstone bridge [4].

This paper provides an analysis of load cell creep by quantifying the individual creep contributions of the counterforce; strain gage backing and adhesive; and strain gage resistive metal foil. The analysis utilizes 14 plane-strain finite element models of a 30-kg aluminum bending beam load cell instrumented with strain gages made with Cu-Ni (constantan) and Ni-Cr (modified Karma) resistive metal foil and with end loop lengths varying from 0.09 to 0.30 mm. Physical measurement of load cell creep is also performed using dead-weight load application of aluminum bending beam load cells corresponding to the finite element models.

2. Analytical and Experimental Methods

The analytical and experimental methods used in this study are described in the following sections.

2.1 Analytical methods

Transducer creep was analyzed using finite element models of a bending beam load cell made with 2024-T4 aluminum and instrumented with strain gages made with Cu-Ni (constantan) and Ni-Cr (modified Karma) resistive metal foil. A photograph of a typical bending beam load cell and a full-bridge strain gage is provided in Fig. 2. This type of load cell is designed so that maximum tension and compression surface strains are developed in the thin

Note: this paper is originally published in Advanced Experimental Mechanics issued by the Japanese Society for Experimental Mechanics.

sections along the top and bottom surfaces of the load cell. In this study the full-bridge strain gage was bonded to the top surface with its 3 mm long sensing grids located directly above each of the thin sections (two grids side-by-side per section).

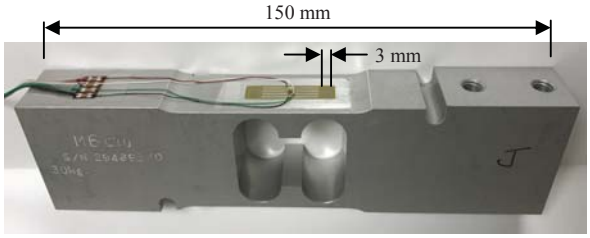

Fig. 2 Aluminum bending beam load cell (capacity 30 kg) with full-bridge strain gage (gage length 3 mm) attached

The strain gages used in this research were constructed using identical manufacturing processes. The conductive element was a rolled metal foil composed of either Cu-Ni (constantan) or Ni-Cr (modified Karma). The metal processing consisted of vacuum induction melting (VIM), casting into cylindrical molds, forging into rectangular cross sections, hot rolling to a thickness of about 3 mm, and cold rolling to a thickness of 5 μm. The cold rolling process included annealing intervals to soften the material, generally after thickness reductions of 50 to 90 percent. The final process annealing thickness was selected to impart about 90 percent thickness reduction in the finished foil [5].

An electrically insulating backing made of 20 μm thick polyimide film was laminated to the foil with epoxy adhesive. The pattern (image) of the strain gage was formed with a photolithographic process by application of a photoresist liquid to the surface of the metal foil, light exposure through an optical mask, and development with a solvent. Typical conductor line dimensions were approximately 25 μm in width by 3 mm in length and with end loop lengths varying from 0.09 to 0.30 mm. Metal removal was by wet process with metal-chloride spray. Final strain gage construction was open-face (without encapsulation). The overall thickness of the open-face strain gages including insulating backing, layer of laminating epoxy, and metal foil was about 25 μm.

Note that after the foil was rolled to its final thickness and prior to application of the electrically insulating backing material, the foil was subjected to a low temperature annealing process at a temperature below 755 K for duration of about 2 hours. This post-rolling annealing process was performed to minimize the temperature sensitivity (thermal output) of the strain gages bonded to aluminum substrates.

A plane-strain finite element model was constructed with consideration of the symmetry of the bending beam load cell. The model represented the top beam of the load cell with displacement constraints applied at one boundary and internal shear forces and moments (force-couple) applied at the other boundary as shown in Fig. 3. A typical portion of the highly refined center regions of the finite element model are shown in Fig. 4. The strain gage portion of the finite element model is depicted in Fig. 5 showing the thickness of the plane-strain elements corresponding to the backing and adhesive, end loop, grid line, and solder tab of the strain gage. This approach was similar to the plane-strain finite element model used by others to study the strain sensitivity and stretchability of silicon-on-polymer strain gages [6]. Elsewhere, three dimensional (3-D) models of strain gages were used to analyze printed ink-jet strain gages applied to printed circuit boards [7]; and the interaction between planar rosette strain gages and relieved stresses using the hole-drilling method [8].

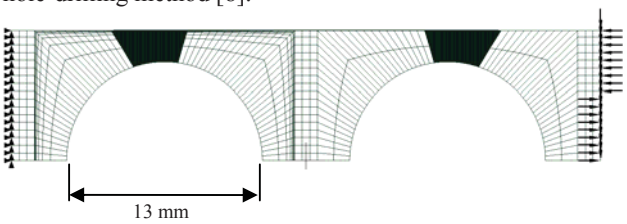

Fig. 3 Finite element model of upper beam of aluminum bending beam load cell (displacement constraints shown on left; applied loads shown on right; highly refined elements shown near center of arched regions in solid black color)

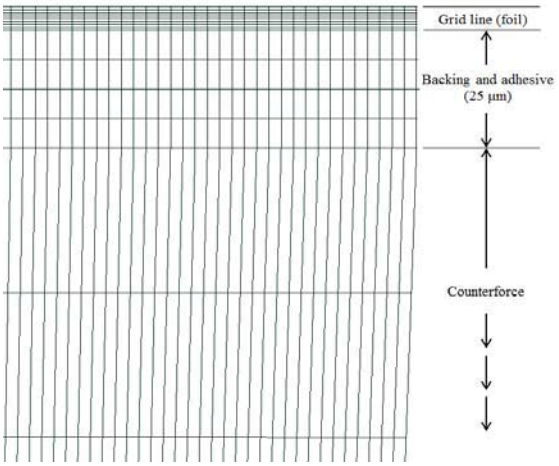

Fig. 4 Portion of highly refined region of finite element model near center of arches (refer to black areas in Fig. 3)

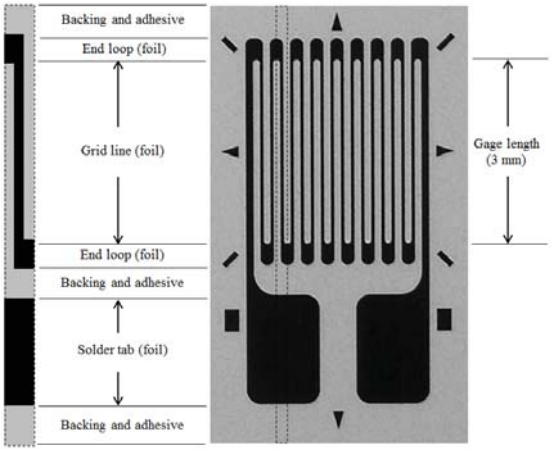

Fig. 5 Strain gage portion of finite element model with plane-strain element widths shown on left corresponding to position on strain gage pattern shown on right

The finite element analysis of the creep developed in a bending beam load cell was based upon the change in elastic response of the counterforce; strain gage backing and adhesive; and strain gage resistive metal foil only at the beginning and end of the loading process; i.e. at time t=0 and t=30 min. Each component of creep was simulated by reducing the individual modulus of elasticities of the aluminum counterforce; strain gage polyimide backing and epoxy adhesive; and strain gage Cu-Ni and Ni-Cr resistive metal foils at time t=30 min from the initial values at time t=0. The creep magnitude of 200 μV/V for 2024-T4 aluminum is reported elsewhere in the characterization and application of creep-resistant alloys [9,10]. The creep magnitudes of 67,000 μV/V for the backing and adhesive; and 310 μV/V for the Cu-Ni resistive metal foil were determined by reducing the modulus of elasticity of these two components until the finite element results were the same as the dead-weight creep test results at times t=0 and t=30 min for Cu-Ni strain gages with end loop lengths of 0.11 and 0.25 mm. The relatively high creep magnitude for polyimide is reported elsewhere in the analysis of creep in viscoelastic polymer [11]; compared to the composite value for backing and adhesive obtained empirically in this analysis. Finally, the creep value of 120 μV/V for Ni-Cr resistive foil was determined by reducing the modulus of elasticity of this component until the finite element result was the same as the dead-weight creep test result at times t=0 and t=30 min for Ni-Cr strain gages with an end loop length of 0.11 mm. Lower creep was expected for Ni-Cr foil due to its higher relative strength compared to Cu-Ni foil [12]. A summary of the modulus of elasticity, Poisson's ratio and creep used for each material is provided in Table 1.

Table 1 Modulus of elasticity, Poisson's ratio and creep

Component	Material	Modulus of Elasticity [GPa]	Poisson's Ratio	Creep [μV/V]
Counterforce	Aluminum	73	0.33	200
Backing/Adhesive	Polyimide/Epoxy	6.9	0.34	67,000
Foil	Cu-Ni	165	0.33	310
Foil	Ni-Cr	221	0.30	120

2.2 Experimental methods

Physical measurement of load cell creep was performed using dead-weight load application of 14 aluminum bending beam load cells corresponding to the finite element models. Each load cell was made of the same batch of 2024-T4 aluminum and had a full-bridge strain gage made of either Cu-Ni or Ni-Cr resistive metal foil 5 μm in thickness and with end loop lengths ranging from 0.09 to 0.30 mm. Test conditions included a constant, applied load of 30 kg for duration of 30 min at ambient (room) temperature. The load corresponded to a full-scale output of about 2.2 mV/V which was equal to a surface strain of approximately 1200 microstrain (μE).

3. Results

Analytical and experimental results for aluminum bending beam load cells instrumented with Cu-Ni and Ni-Cr strain gages are superimposed in a plot of creep versus strain gage end loop length provided in Fig. 6. The well-known and expected relationship between load cell creep and length of the strain gage end loop is seen in both the finite element and dead-weight test results as creep increased positively from nearly -600 μV/V for an end loop length of 0.09 mm to about 300 μV/V for an end loop length of 0.30 mm.

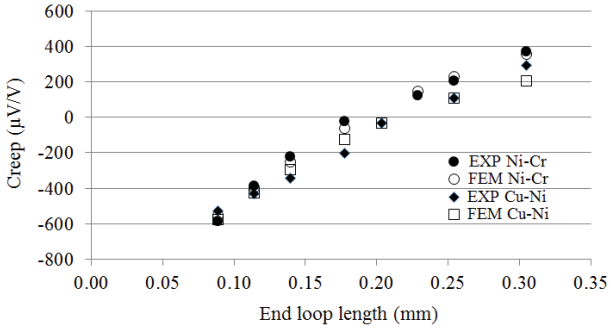

Fig. 6 Bending beam load cell creep from experiments (EXP) and finite element models (FEM)

Good correlation is seen between finite element analysis and dead-weight creep test results with the maximum difference between the two methods of about 100 μV/V across the range of end loop lengths. Minimum bending beam load cell creep of -22 and -30 μV/V was achieved for strain gages made of Ni-Cr and Cu-Ni resistive metal foil with end loop lengths of 0.18 and 0.20 mm, respectively. This is consistent with the relative creep contributions for the two resistive metal foils (120 and 310 μV/V for Ni-Cr and Cu-Ni foil respectively).

4. Conclusions

A brief summary of the findings in this paper follows:

1. It is possible to obtain good correlation between finite element analysis and dead-weight creep test results of bending beam load cells by incorporating the individual creep contributions of the counterforce; strain gage backing and adhesive; and strain gage resistive metal foil.
2. Using similar methodology a variety of additional analyses of transducer creep would appear to be feasible such as: the effect of load cell design (column, shear, torque, etc.); strain gage design (encapsulation, gage length, grid line spacing, foil thickness, etc.); and materials of construction.

References

[1] Organisation Internationale de Metrologie Legale: *International Recommendation OIML R 76* (edition 1992 E), Grande Imprimerie de Troyes (1994), 1-83.

[2] Kieffer, T. P., Watson, R. B., Showalter, R. L. and Harris, S. K.: Strain gage with off axis creep compensation feature, *United States Patent Application Publication 0288795A1*, (2006).

[3] Kreuzer, M.: Strain gages for transducers, *Germany Patent Application Publication 102006021423A1*, (2007).

[4] Zandman, F., Watson, R. B. and Kieffer, T. P.: Circuit compensation in strain gage based transducers, *United States Patent 8161829B2*, (2012).

[5] Robinson, M.: Strain gage materials processing, metallurgy, and manufacture, *Exp. Tech.*, **30**-1 (2006), 42-46.
[6] Shixuan, Y. and Nanshu, L.: Gauge factor and stretchability of silicon-on-polymer strain gauges, *Sensors*, **13**-1 (2013), 8577-8594.
[7] Silva, E. R., Oliveira, W. C., Arruda, L. O., Bonadiman, R., Quintero, J., Mancuso, R. and Silva Neto, J. M.: Finite element simulation of inkjet printed strain gage on polyimide substrates applied to flexible boards, Proc. 11th Electronics Packaging Technology Conference IEEE, **2**-1 (2009), 607-611.
[8] Sarga, P., Senko, P. and Trebuna, F.: Analysis of influence of strain gage rosette on relieved strain, *Am. J. Mech. Eng.*, **1**-7 (2013), 309–312.
[9] Robinson, J. S., Cudd, R. L. and Evans, J. T.: Creep resistant aluminum alloys and their applications, *Mat. Sci. and Tech.*, **19**-2 (2003), 143-155.
[10] Liu, L., Zhan, L. and Li, W.: Creep aging behavior characterization of 2219 aluminium alloy, *J. Metals*, **6**-7 (2016), 146-155.
[11] Jansons, J., Aniskevich, A. and Pahze, L.: Analysis of reversible and irreversible strains in the creep of a nonlinear viscoelastic polymer, *Mech. Comp. Matl.*, **48**-2 (2012), 209-216.
[12] Deibler, L. A.: Room temperature creep in metals and alloys, *Sandia Report SAND2014-17935*, Sandia National Laboratories (2014), 1-48.